Time-domain system identification using fractional models from non-zero initial conditions applied to Li-ion Batteries

Abderrahmane Adel, Olivier Briat, Rachid Malti

Signal Processing

Time-domain system identification using fractional models from non-zero initial conditions applied to Li-ion Batteries

--Manuscript Draft--

Manuscript Number:	SIGPRO-D-24-02726
Article Type:	Research Paper
Keywords:	System identification, Fractional order equivalent circuit model, Batteries, Parameters estimation, Time-domain identification.
Corresponding Author:	Abderrahmane Adel, Ph.D. Candidate Universite de Bordeaux Talence, FRANCE
First Author:	Abderrahmane Adel, Ph.D. Candidate
Order of Authors:	Abderrahmane Adel, Ph.D. Candidate
	Rachid Malti, Professor
	Olivier Briat, Professor
Abstract:	The main contribution of this paper is to present two distinct algorithms for fractional system identification using non-zero initial conditions, by assuming the input signal prior to $t = 0$ and the input/output signals after $t = 0$ known. Addressing this problem is particularly important, in the context of short data acquisition, mainly for two reasons (i) the effect of free response is important compared to the forced one (ii) time-domain response of fractional systems converge polynomially, as compared to the exponential convergence of rational systems. The first developed algorithm uses a two-stage iterative procedure that computes system forced response at the upper stage, and system parameters at the lower stage. The second one relies on an output error model, estimating parameters due to the simultaneous contribution of system free and forced responses. The efficacy of both algorithms is first assessed using Monte Carlo simulations with significant signal to noise ratios. The proposed algorithms, applied to the identification of commercial Li-ion battery cells, allow solving a technical issue: straightforward data acquisition whatever the past history of the cells, i.e. the cells need not be in a completely relaxed state prior to collecting data, contrary to the actual practice.

Highlights

- Two novel algorithms developed for fractional system identification with non-zero initial conditions.
- The first algorithm uses a two-stage process, separating free and forced responses for accuracy.
- The second algorithm estimates parameters by simultaneously incorporating free and forced responses.
- Both algorithms validated experimentally and with Monte Carlo simulations on Li-ion batteries.
- Application to the identification of Li-ion batteries by eliminating the relaxation time.

Time-domain system identification using fractional models from non-zero initial conditions applied to Li-ion Batteries

Abderrahmane Adel*, Rachid Malti, Olivier Briat

[a] *Univ. Bordeaux, CNRS, Bordeaux-INP, IMS – UMR 5218, 351, cours de la Libération, Talence, 33400, France*

Abstract

The main contribution of this paper is to present two distinct algorithms for fractional system identification using non-zero initial conditions, by assuming the input signal prior to $t = 0$ and the input/output signals after $t = 0$ known. Addressing this problem is particularly important, in the context of short data acquisition, mainly for two reasons (i) the effect of free response is important compared to the forced one (ii) time-domain response of fractional systems converge polynomially, as compared to the exponential convergence of rational systems. The first developed algorithm uses a two-stage iterative procedure that computes system forced response at the upper stage, and system parameters at the lower stage. The second one relies on an output error model, estimating parameters due to the simultaneous contribution of system free and forced responses. The efficacy of both algorithms is first assessed using Monte Carlo simulations with significant signal to noise ratios. The proposed algorithms, applied to the identification of commercial Li-ion battery cells, allow solving a technical issue: straightforward data acquisition whatever the past history of the cells, i.e. the cells need not be in a completely relaxed state (with zero initial conditions) prior to collecting data, contrary to the actual practice.

Keywords: System identification, Fractional order equivalent circuit model,

*Corresponding author

Email addresses: abderrahmane.adel@ims-bordeaux.fr (Abderrahmane Adel), rachid.malti@ims-bordeaux.fr (Rachid Malti), olivier.briat@ims-bordeaux.fr (Olivier Briat)

Batteries, Parameters estimation, Time-domain identification.

1. Introduction

There are various system identification methods that use fractional models and zero initial conditions [1, 2, 3, 4]. The initial conditions are often assumed to be zero for the sake of simplicity, which might have a limited effect when the amount of data is big. However, in case of small data acquisition, ignoring initial conditions leads to significantly biased parameter estimation when the initial conditions are varied [5, 6, 7].

Handling initial conditions in fractional calculus has been solved in the general case by [5, 6] (see also the excellent book by the same authors [8]). However, to the best of the authors' knowledge, only limited research has addressed system identification with non-zero initial conditions, despite its relevance in some practical applications. This gap, filled in this paper, has interesting applications like in the case of modeling lithium-ion batteries for the sake of predicting their State Of Charge (SOC) and State Of Health (SOH) [9]. When battery cells are in operating conditions or brought intentionally to a certain SOC-Level, usually a quite long relaxation period is observed for the effect of initial conditions to vanish, prior to collecting identification data [10, 11, 12, 13].

This paper presents two system identification algorithms able to compute unbiased parameters in presence of non-zero initial conditions. The paper is organized as follows. First of all, some basics on handling initial conditions for rational and fractional systems are recalled and the difficulty of handling the fractional case is explained. Then, the problem is formulated under some hypotheses and the main contributions of the paper are stated. The case-study application is also introduced in this section prior to describing the main contribution of the paper with two developed algorithms in section 2. Their performance is tested in Monte Carlo simulation in section 3 and applied to a real case study in section 4 before concluding.

1.1. Initial conditions in fractional calculus

Consider a linear system (rational or fractional) characterized by a transfer function $H(s)$. Basically, its time-domain response to an input signal $u(t)$ is governed by the following convolution integral, which clearly points out the contribution (to the future output $y(t)$ for $t \geq 0$) of both the free

response due to $u(t)$ for $t < 0$, and the forced response due to $u(t)$ for $t \geq 0$ [8]:

$$y(t) = \underbrace{\int_a^0 h(t-x)u(x)\,\mathrm{d}x}_{\varphi(t)\equiv \text{ free response}} + \underbrace{\int_0^t h(t-x)u(x)\,\mathrm{d}x}_{\text{forced response}} \tag{1}$$

The concept of free response, known also as the initial condition response, refers to how a system reacts to displacements of its variables from their equilibrium position. In rational (integer-order) systems, it is well established that the initial values are all defined at $t = 0$, whatever the past trajectories ($t < 0$) of system variables which allowed reaching these initial values. Take for example the RC-circuit of Fig. 1 subject to the input signal, plotted in red, in Fig.2. Then, its transfer function, computed from the circuit impedance, writes:

$$H(s) = \frac{Y(s)}{U(s)} = \frac{1}{1+\tau s} \tag{2}$$

where $Y(s)$ and $U(s)$ are the Laplace transforms of the voltages $y(t)$ and $u(t)$, indicated in Fig.1, and $\tau = RC$. By computing the inverse Laplace transform of (2), one may obtain the impulse response $h(t) = \frac{1}{\tau}\exp(-t/\tau)$, and consequently reduce (1) to:

$$y(t) = \underbrace{y_0 \exp\left(\frac{-t}{\tau}\right)}_{\text{free response}} + \underbrace{1 - \exp\left(\frac{-t}{\tau}\right)}_{\text{forced response}} \tag{3}$$

where $y_0 = (1 - \exp(a/\tau))$ represents the initial condition in this example. It is fully characterized by the initial value $y(0) = y_0$, whatever the possible past trajectories of $y(t)$, $t < 0$. When dealing with fractional differential equations, extra care is necessary due to their infinite memory behavior and the polynomial convergence of their free response as compared to the exponential convergence of rational systems [14, 15]. The free response not only depends on the initial values of system variables but also on the past trajectory of these variables. Instead of a finite number of initial conditions, fractional systems require using an infinite number of initial values, usually gathered in an initialization function. Two kinds of initialization functions are proposed in the literature. The first one is based on a time-domain "history-function" [16, 5] and the second one on the frequency-domain "infinite state approach" [6]. Both approaches show similar results on numerous examples [17]. They

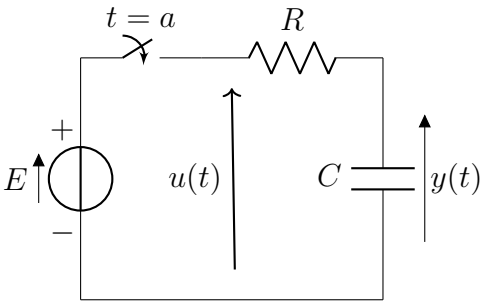

Figure 1: RC-circuit

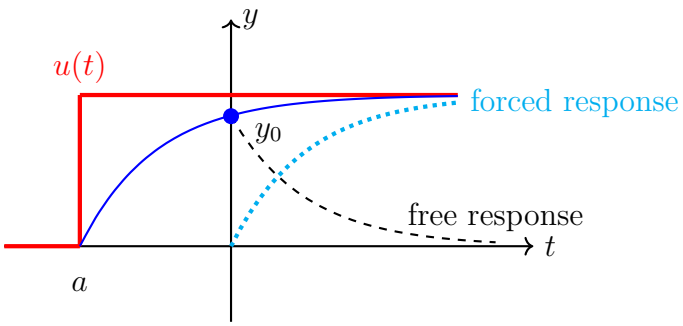

Figure 2: Input signal $u(t)$ in red and output signal $y(t)$ in blue, the blue dot indicates the initial condition y_0.

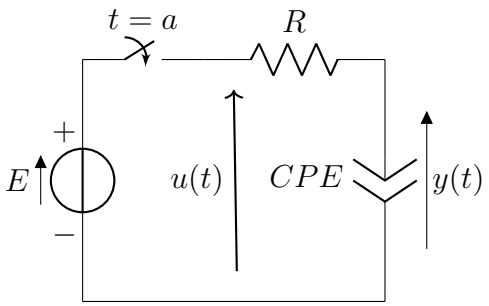

Figure 3: $R-$CPE-circuit

are presented in the sequel on a simple example borrowed from [17]. Consider the circuit of Fig.3 with a constant phase element (CPE) having the impedance $\frac{1}{Qs^\alpha}$, with $0 < \alpha < 1$. The case $\alpha = 1$ describes a capacitor, $\alpha = 0$ a resistor, and $\alpha = 0.5$ Warburg impedance encountered in battery modeling [18, 19]. This circuit is governed by the fractional differential equation:

$$\tau_c \frac{\mathrm{d}^\alpha}{\mathrm{d}t^\alpha} y(t) + y(t) = u(t) \tag{4}$$

where $\tau_c = RQ$. Its transfer function may be computed from (4):

$$H(s) = \frac{Y(s)}{U(s)} = \frac{1}{1 + \tau_c s^\alpha} \tag{5}$$

Let $h(t) = \mathscr{L}^{-1}\{H(s)\}$ be the impulse response of the new circuit. The convolution product (1) yet holds for fractional systems. However, it becomes more difficult to compute the free response integral in the fractional case. The main approach developed in the literature is based on the infinite state approach.

1.1.1. Infinite-state approach (Trigeassou and Maamri)

In this approach [6], the free response of the fractional differential equation (4), is solution of the homogeneous equation (without the input $u(t)$, for $t < 0$):

$$\tau_c \frac{\mathrm{d}^\alpha}{\mathrm{d}t^\alpha} y(t) + y(t) = u'(t) \text{ with } u'(t) = \begin{cases} u(t) \text{ for } t < 0 \\ 0 \text{ for } t \geq 0 \end{cases} \tag{6}$$

It may be expressed as a distributed differential system:

$$\begin{cases} \dfrac{\partial z(\omega,t)}{\partial t} = -\omega z(\omega,t) - \dfrac{1}{\tau_c} y(t) \\ y(t) = \int_0^\infty \mu_\alpha(\omega) z(\omega,t)\,\mathrm{d}\omega \end{cases} \tag{7}$$

where $\mu(\omega)$ is a weighting function defined in the case of an integrator by

$$\mu_\alpha(\omega) = \frac{\sin(\alpha\pi)}{\pi}\omega^{-\alpha} \tag{8}$$

The distributed initial conditions are gathered in the function $z(\omega, 0)$, which depends on all the frequencies ω and verifies the initial value:

$$y(0) = \int_0^\infty \mu_\alpha(\omega) z(\omega,0)\,\mathrm{d}\omega \tag{9}$$

1.1.2. History-function (Hartley and Lorenzo)

The history function approach, due to [16, 5], corresponds to the application of the input/output methodology. The authors compute the convolution integral

$$\varphi(t) = \int_a^0 h(t-x)u(x)\,\mathrm{d}x \tag{10}$$

in the case of elementary systems of the first kind [20] by setting constant and/or ramp history functions in order to be able to formulate analytical expressions, based on the Mittag-Leffler and the incomplete Gamma functions, of $\varphi(t)$ and its Laplace transform.

1.2. Problem formulation

The problem addressed in this paper is related to system identification using linear fractional models from non-zero initial conditions under the following hypothesis:

(H1) The past ($t < 0$) and the future ($t \geq 0$) of the input signal $u(t)$ are known.

(H2) Only the future ($t \geq 0$) of the output signal $y(t)$ is known.

(H3) Model structure is known.

(H4) Input signal is noise-free ; output signal may be affected by noise.

Hence, model parameters and differentiation orders are unknown and estimated. When model structure is unknown (i.e. when (H3) is invalidated), searching for the model structure may be achieved by using some AIC-like criteria. If input data are noisy (hypothesis (H4) invalidated), then the proposed algorithms may be extended by using Error-In-Variables (EIV) methodology.

1.3. Main contributions

The main contributions of this paper are summarized below.

- Two methods are developed to solve the problem formulated in 1.2.
  - The first one is based on a two stage algorithm allowing separation of the free and the forced responses on each stage,
  - the second one is based on a straightforward parameter estimation taking into account simultaneously the free and the forced responses.
- The accuracy and the computational efficiency of both methods is assessed.
- A technical issue related to Li-ion batteries is solved. It avoids waiting for long periods of time for the batteries to be in a completely relaxed state, with a vanished free response, prior to collecting identification/validation data.
- Experimental validation is conducted on three commercial batteries.

Through the development and validation of these innovative techniques, this study aims to advance the field of battery characterization with broader applications and improved performance.

1.4. Motivations in Li-ion Battery modeling

One of the most used system identification techniques is based on Electrochemical Impedance Spectroscopy (EIS) which consists in performing a harmonic analysis with a sine excitation current and measuring the output voltage across the electrodes. Then, the current and voltage signals are used for computing the impedance spectrum, fitted to a fractional order equivalent circuit model (FO-ECM) [21]. A typical impedance spectrum of a commercial battery cell is plotted in Fig.4 . Low frequencies $0.1 < f < 1$

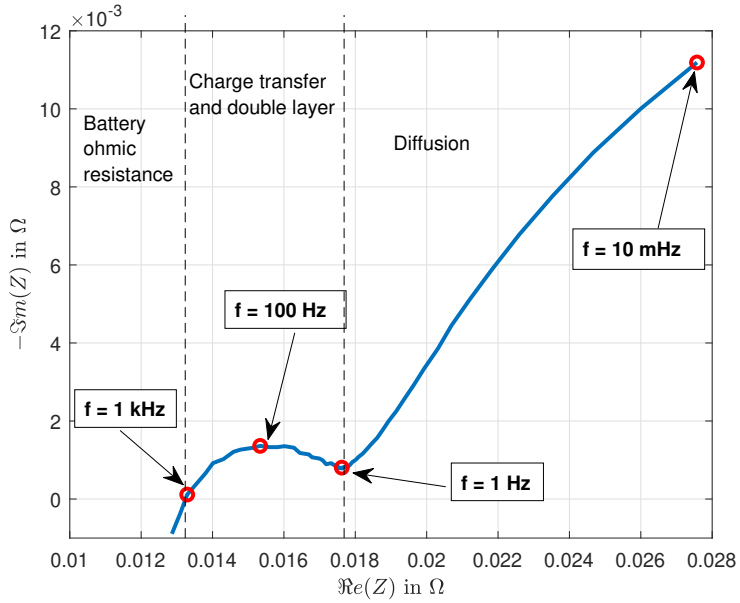

Figure 4: Nyquist plot of a Samsung "INR18650-25R" battery impedance measured in GEIS mode at SOC 80%, 25°C.

Hz, characterizing the diffusive Warburg phenomenon, may be modeled by a Constant Phase Element, CPE_2, in Fig.5 which impedance is:

$$Z_d(s) = CPE_2 = \frac{1}{Q_d s^\beta} \tag{11}$$

where Q_d is a coefficient, and β a differentiation order equal to 0.5 when Warburg impedance is considered and might be further adjusted from input-output data. Mid-range frequencies $1 < f < 10^3$ Hz, related to charge transfer phenomenon, are usually modeled by another constant phase element, CPE_1, see e.g. [22], characterized by a constant Q_{dl} and a differentiation order α, in parallel with the resistor R_{ct}:

$$\begin{aligned} Z_{ct}(s) &= R_{ct} \parallel CPE_1, \quad \text{with} \quad CPE_1 = \frac{1}{Q_{dl} s^\alpha} \\ Z_{ct}(s) &= \frac{R_{ct}}{1 + R_{ct} Q_{dl} s^\alpha} \end{aligned} \tag{12}$$

The high frequency $f \approx 10^3$Hz, corresponding to the intersection of the impedance with the real axis in Fig.5, corresponds to the ohmic resistor

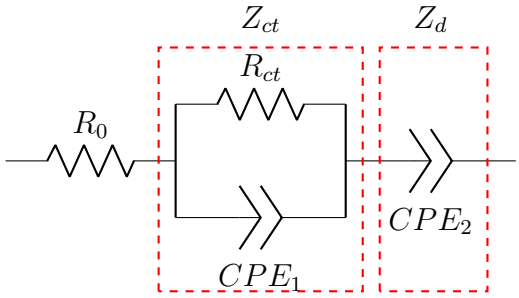

Figure 5: Global impedance model of the Li-ion battery. The rectangle highlights Z_{ct}, consisting of R_{ct} and CPE_1.

of the battery, R_0 in Fig.5. Beyond this frequency, $f > 10^3$Hz, an inductive phenomenon appears characterized in Fig.4 by negative values of the y-coordinate (or positive values of $\mathscr{I}m(z)$). The inductive phenomenon is not considered in this paper and the batteries are modeled in a frequency range up to 10^3Hz. Hence, the overall impedance of the Li-ion battery, as illustrated in Fig.5, is the combination of the three considered effects:

$$\begin{aligned} Z(s) &= R_0 + Z_{ct}(s) + Z_d(s) \\ &= R_0 + \frac{R_{ct}}{1 + R_{ct}Q_{dl}s^{\alpha}} + \frac{1}{Q_d s^{\beta}} \\ &= \frac{R_0 R_{ct} Q_{dl}^{a_0} s^{\beta+\alpha} + R_0 + R_{ct}^{a_1} s^{\beta} + \frac{R_{ct}Q_{dl}}{Q_d} s^{\alpha} + \frac{1}{Q_d}}{R_{ct}Q_{dl}s^{\beta+\alpha} + s^{\beta}}. \end{aligned} \tag{13}$$

Let battery parameters be gathered in a vector

$$\theta = [R_0, R_{ct}, Q_{dl}, \alpha, Q_d, \beta]^T. \tag{14}$$

The fractional-order equivalent circuit model (FO-ECM) with two constant phase elements, as in (13) and in Fig.5, has been used in [21] to study the structural identifiability of such models by solving algebraic equations. One of the major issues with EIS data is the long acquisition time, as the method sweeps through 5 decades of frequencies ranging from 0.01Hz to 1KHz (see e.g. Fig.4). Such a long acquisition time may affect the SOC-level. An interesting alternative to EIS data acquisition consists in using chronopotentiometry time-domain measurements, which consists in applying an excitation current (such as a pseudo-random-binary-signal (PRBS)) and measuring the

output voltage across the electrodes. Multiple references [23, 24, 25, 21, 26] suggest using the FO-ECM developed in section 1.4 as impedance models and time domain data. Fractional models may be simulated in the time domain using [27] approximation of fractional operators, implemented in the CRONE Toolbox [28]. [24] use an output-error model combined to a non-linear programming techniques to compute the model parameters. Such techniques effectively reduce aquisition time [24, 25]; however, the battery cells yet need be at a relaxed state, as explained below.

Impact of the relaxation period

To obtain accurate impedance models, frequency-domain and/or time-domain measurements require thermodynamic steady-state conditions, which are usually obtained after a significant relaxation time when the battery is active or brought to a given SOC. Indeed, voltage relaxation (VR) stems from an electrochemical process occurring after interrupting the current flow into or from the battery which results in a gradient of lithium ions through electrodes [29]. The bigger the relaxation time, the lesser the gradient of ions across the electrodes. Various references [11, 12, 13] study the impact of the relaxation time in modeling Li-ion batteries. [11] show the influence of relaxation-time on the time-domain responses to a prescribed input. [13] explore the variation of cell impedance for different relaxation periods (0, 30, 60, 180, 300, 420)mn, based Potentiostatic-EIS (on voltage variations at the input and current measurement at the output). It is highlighted in the aforementioned paper the necessity to wait for a sufficiently long period (up to 420mn) for a battery cell [13] to be completely relaxed. [12] study the influence of relaxation time on 5 different commercial batteries, stressing the fact that the relaxation time might be as big as 900mn for certain cells. Further, characterizing batteries at different SOC-levels requires the battery to be in a relaxed state every time it is brought to the desired SOC-level, whatever the acquisition: in frequency-domain or time-domain.

This paper aims at developing system identification algorithms able to estimate parameters, using non-relaxed Input-Output data, which constitutes an important breakthrough in Li-ion batteries identification, eliminating relaxation time usually observed for the free response to vanish prior to data acquisition.

2. Contributions to system identification with non-zero initial conditions

Consider a linear fractional system characterized by a transfer function:

$$H(s,\theta) = \frac{\sum_{i=0}^{M} b_i s^{\beta_i}}{1 + \sum_{j=1}^{N} a_j s^{\alpha_j}}. \tag{15}$$

or its impulse response $h(t,\theta) = \mathscr{L}^{-1}\{H(s,\theta)\}$, where the parameter vector

$$\theta = \begin{bmatrix} \rho \\ \mu \end{bmatrix} \tag{16}$$

is composed of a vector of $N+M+1$ transfer function coefficients,

$$\rho = [b_0, b_1, \ldots, \ b_M, a_1, \ldots, a_N]^{\mathrm{T}}, \tag{17}$$

and additionally a vector of $N+M+1$ ordered differentiation orders,

$$\mu = [\beta_0, \ldots, \beta_M, \alpha_1, \ldots, \alpha_N]^{\mathrm{T}}. \tag{18}$$

System identification using fractional models with zero initial conditions have been treated in the litterature, mainly in an output error context [30, 31], or using least squares estimates [22] and the optimal instrumental variable [4]. In the output error context, model parameters are computed by minimizing the L_2-norm squared

$$J(\theta) = \|\epsilon(t,\theta)\|^2 \tag{19}$$

of the output error:

$$\epsilon(t,\theta) = y(t) - \hat{y}(t,\theta). \tag{20}$$

as illustrated in Fig.6. In case of the impedance model (13), the parameter vector θ is defined in (14). Equation (19) can be written in a discretized form, based on trapezoidal rule:

$$J(\theta) \approx T_s \sum_{k=0}^{K-1} \epsilon^2(kT_s,\theta) = T_s E^T(\theta) E(\theta) \tag{21}$$

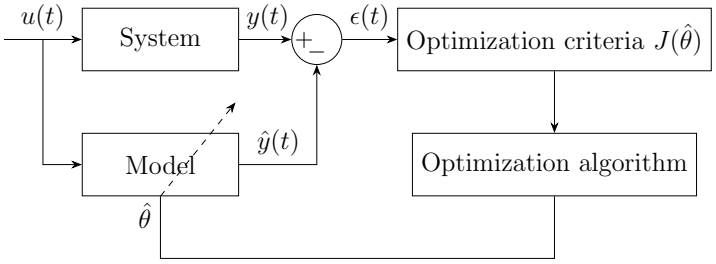

Figure 6: Output error model.

where T_s is the sampling period, K the total number of samples and the error vector $E(\theta) = [\epsilon(0,\theta), \ldots, \epsilon(K-1,\theta)]^T$

The optimal parameter vector, minimizing (21),

$$\hat{\theta} = \arg\min_{\theta} J(\theta), \tag{22}$$

is usually obtained using a nonlinear optimization algorithm. The iterative Levenberg-Marquardt algorithm [32] is often used. In case of rational systems, when system output is a combination of a free and a forced response, then the initial conditions, constituted of consecutive derivatives of y up to system order minus one $(n-1)$ all evaluated at $t = 0$, gathered in $\mathscr{Y}_0 = [y(0), \frac{\mathrm{d}y}{\mathrm{d}t}(0), \ldots, \frac{\mathrm{d}^{n-1}y}{\mathrm{d}t^{n-1}}(0)]$, may be estimated along with system parameters

$$(\hat{\theta}, \mathscr{Y}_0) = \arg\min_{\theta, \mathscr{Y}_0} J(\theta, \mathscr{Y}_0), \tag{23}$$

by minimizing the quadratique criterion

$$J(\theta, \mathscr{Y}_0) = \|\epsilon(t, \theta, \mathscr{Y}_0)\|^2 = \|y(t) - \hat{y}(t, \theta, \mathscr{Y}_0)\|^2. \tag{24}$$

Take for instance, the RC-circuit of Fig.1 and its global response in (3), then the quadratic error may be expressed in terms of the initial condition y_0 along with the transfer function parameter τ:

$$J(\tau, y_0) = \|\epsilon(t, \tau, y_0)\|^2 = \|y(t) - \hat{y}(t, \tau, y_0)\|^2. \tag{25}$$

Such a formulation becomes impossible for fractional systems, because the free response depends on an infinite number of initial conditions, as explained in section 1.1. Hence, this section introduces two novel approaches for parameter estimation of fractional models with non zero initial conditions: the separate free and forced response method and the simultaneous free and forced response method.

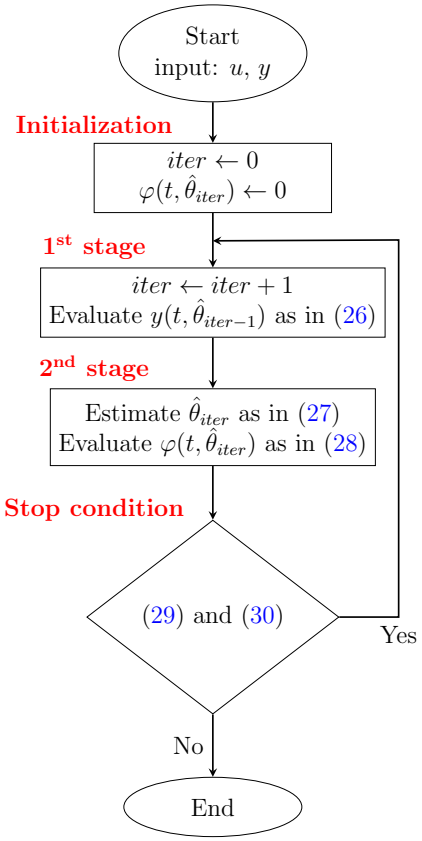

Figure 7: Flowchart of the 1st method (separate free and forced responses) estimating the fractional model of the battery considering historical data.

2.1. Parameter estimation using separate free and forced responses

In this section, an iterative two-stage algorithm is proposed to minimize the output error when initial conditions are unknown. Two-stage algorithms, have been used in various domains. For instance, in the context of structure identification of Polynomial NARX models [33] utilize a two-stage algorithm with at the first stage coarsely identifies the model structure, and the second stage iteratively refines it. [4] employ a two-stage algorithm, estimating transfer function parameters using least squares at one stage and differentiation orders using a gradient-based algorithm at the other stage. The proposed algorithm, sketched in Fig.7, is detailed below.

2.1.1. Initialization

Start by initializing *iter* at 0, and consider that the free response equals zero (the undetermined $\hat{\theta}_0$ is not required).

2.1.2. First stage

The main idea is to subtract from the output signal, at the first stage and from the second iteration on, the free response and to keep only the forced one:

$$y(t, \hat{\theta}_{iter-1}) \leftarrow y(t) - \varphi(t, \hat{\theta}_{iter-1}) \tag{26}$$

At the very first iteration, as $\varphi(t, \hat{\theta}_0) = 0$, system output is considered to be only due to the forced response which is non-consistant, yielding biased results, in presence of free response. The estimation is less biased as the number of iterations gets bigger[1].

2.1.3. Second stage

The basic idea of the second stage is to compute the parameter vector and once the model known, compute its free response. Hence, estimate the parameter vector $\hat{\theta}_{iter}$ using the levenberg-Marquardt algorithm from (19)-(22) by considering $y(t, \hat{\theta}_{iter-1})$ instead of $y(t)$ in (20):

$$\hat{\theta}_{iter} = \arg\min_{\theta} J(\theta). \tag{27}$$

Once $\hat{\theta}_{iter}$ known, the transfer function and its impulse response are completely defined $\hat{H}(s, \hat{\theta}_{iter}) = \mathscr{L}\{\hat{h}(t, \hat{\theta}_{iter})\}$. Hence model free response, is computed:

$$\varphi(t, \hat{\theta}_{iter}) = \underbrace{\int_a^0 \hat{h}(t - x, \hat{\theta}_{iter}) u(x)\, \mathrm{d}x}_{\text{free response}}, \tag{28}$$

and the algorithm is iterated back to the first stage by separating the free response from the whole system response as in (26).

[1] See section 2.1.5 for convergence notes.

2.1.4. Convergence test

The procedure is iterated as long as a norm of the difference between two successive normalized estimates is greater than a threshold ϵ (here the ℓ_1-norm is used):

$$\sum_{\ell=1}^{L} \left| \frac{\hat{\theta}^{\ell}_{iter} - \hat{\theta}^{\ell}_{iter-1}}{\hat{\theta}^{\ell}_{iter-1}} \right| > \epsilon, \tag{29}$$

or a maximum number of iterations is not reached yet

$$iter \leq iter_{max}. \tag{30}$$

here $\ell = 1, 2, \ldots, L$ represents the number of estimated parameters, $\hat{\theta}^{\ell}_{iter}$ is the ℓth element of the estimated parameter vector at the iteration $iter$.

2.1.5. Convergence notes

To the best of authors' knowledge, convergence of such two-stage algorithms cannot be proven, although it is noted in multiple references (see e.g. [34, 35, 4]) that they do often converge to a minimum.

2.2. Parameter estimation using simultaneous free and forced responses

In this section, a second algorithm is suggested, estimating model parameters on the basis of a simultaneous estimation of the free and the forced responses by considering straightforwardly system whole response (1). The algorithm, illustrated in Fig. 8, begins by initializing the parameter vector θ. Then, the global system response, constituted of the free and forced responses, is computed:

$$y(t,\theta) \leftarrow \underbrace{\int_{a}^{0} h(t-x,\theta)u(x)\,\mathrm{d}x}_{\varphi(t,\theta) \equiv \text{ free response}} + \underbrace{\int_{0}^{t} h(t-x,\theta)u(x)\,\mathrm{d}x}_{\text{forced response}} \tag{31}$$

where $h(t-x,\theta)$ represents the system impulse response parameterized by the model parameter vector θ. Once the total system output is computed, the algorithm proceeds by estimating the parameter vector $\hat{\theta}$ using the levenberg-Marquardt algorithm from (19)-(22) by considering $y(t,\theta)$ of (31) instead of $y(t)$:

$$\hat{\theta} = \arg\min_{\theta} J(\theta). \tag{32}$$

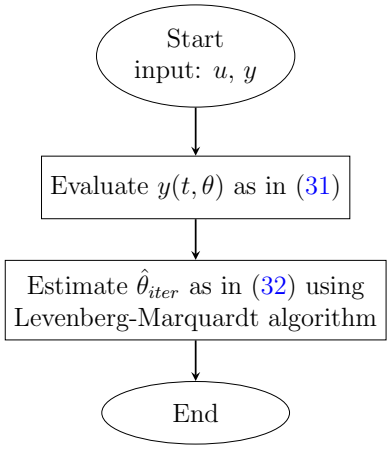

Figure 8: Flowchart of the 2nd method (simultaneous free and forced responses) estimating the fractional model of the battery considering historical data.

This method allows simultaneous consideration of both free and forced responses in estimating system fractional model, making it particularly suitable for applications like battery modeling where the past history (free response) significantly influences future behavior.

3. Simulation example on a battery impedance model

The objective of this section is to validate both algorithms described in sections 2.1 and 2.2 on a simulation example with non-zero initial conditions. The advantages of a simulation example are (i) evaluating the effectiveness of the method, by testing whether the true parameters are recovered (ii) using Monte Carlo simulation, with 100 runs, to determine the accuracy of parameter estimation algorithms and their robustness in presence of noisy data with a signal to noise ration of 20dB and then 10dB.

3.1. Simulation example of a battery system

The battery model structure (13) is chosen by setting its parameters to values close to experimental ones computed in [26]:

$$R_0 = 13.8\,\mathrm{m\Omega}, \quad Q_{dl} = 6.47\,\mathrm{F}\cdot\mathrm{s}^{1-\alpha}, \quad \alpha = 0.7,$$
$$R_{ct} = 5\,\mathrm{m\Omega}, \quad Q_d = 333\,\mathrm{F}\cdot\mathrm{s}^{1-\beta}, \quad \beta = 0.6.$$

The input current signal, plotted in Fig. 9, is constituted of a historical input signal (for $t < 0$) a charging sequence with a current amplitude of 1A and

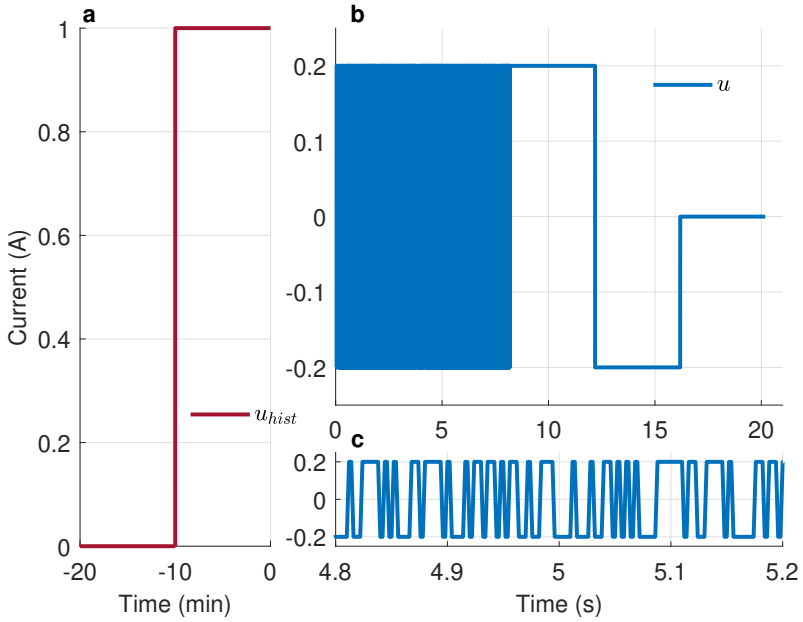

Figure 9: (a) Historical input signal. (b) Input signal used for system characterization. (c) Zoom on the PRBS signal.

a duration of ten minutes, followed by an identification signal constituted of fast and slow dynamics. An 8-second Pseudo-Random Binary Sequence (PRBS) is implemented for current excitation, with an amplitude of 200 mA, followed by an 8-second charge/discharge sequence with a current alternating between −200 and 200 mA. Finally, a 4 seconds rest period is observed. The entire sequence lasts 20 seconds.

3.2. Results of both algorithms

The results are plotted in Fig. 10 and further illustrated in Table 1 which show that the parameters converge for both algorithms to the true values with very low standard deviation.

For a SNR of 20 dB. Both methods, described in section 2.2 and 2.1, converge for all simulations with a 100% convergence rate. Moreover, both algorithms provide accurate parameter estimates, with low standard deviations for all parameters, indicating good precision under moderate noise conditions.

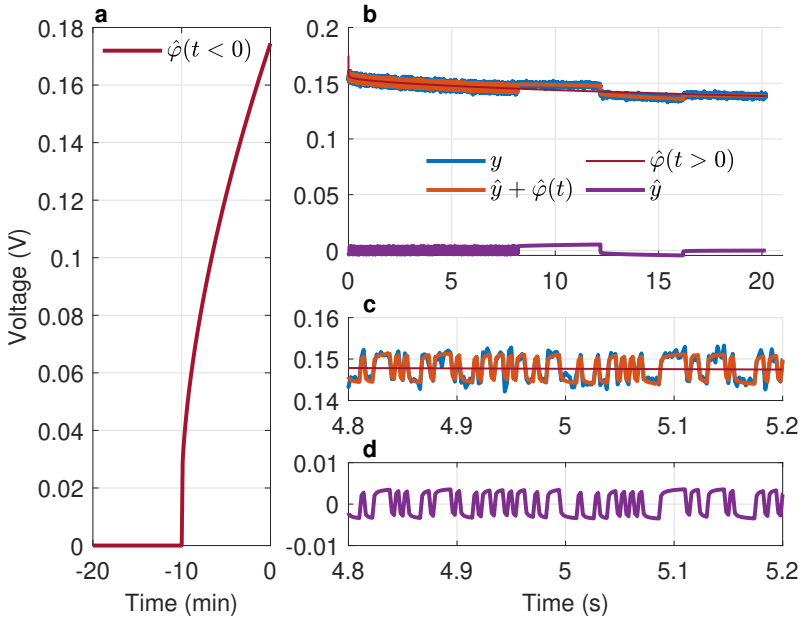

Figure 10: Simulated battery model without relaxation period: (a) Free response. (b) Battery model and estimated model responses. (c) Zoom of the battery model and estimated model responses. (d) Zoom of the forced response.

Table 1: A comparison of parameter estimation accuracy with and without a relaxation period of 60 min using both algorithms in case of SNR equal to 20dB and 10dB.

T_{relax}		Algo. section 2.1				Algo. section 2.2			
signal to noise ration SNR		20dB		10dB		20dB		10dB	
Parameter	True	θ	$\hat{\sigma}_\theta$	θ	$\hat{\sigma}_\theta$	θ	$\hat{\sigma}_\theta$	θ	$\hat{\sigma}_\theta$
R_0 (mΩ)	13.8	13.791	0.015	13.762	0.021	13.802	0.009	13.814	0.017
R_{ct} (mΩ)	5	5.11	0.08	26.34	4.12	5.01	0.01	5.07	0.02
Q_{dl} (F$\cdot$s$^{1-\alpha}$)	6.47	6.49	0.44	1.42	0.85	6.46	0.18	6.49	0.47
α	0.7	0.7041	0.0134	0.7108	0.0201	0.7012	0.0135	0.7083	0.0141
Q_d (F$\cdot$s$^{1-\beta}$)	333	320	10	287	26	334	3	330	8
β	0.6	0.6031	0.0044	0.5921	0.0065	0.6011	0.0041	0.6034	0.0043
Convergence		100/100		81/100		100/100		100/100	
Non convergence		-		19/100		-		-	

Table 2: Characteristics of three commercial battery cells used in this experiment.

Cell ref	**SGg**	**LGb**	**SGp**
Reference	INR1865025R	INR18650HG2	ICR1865026F
Manufacturer	Samsung	LG Chem	Samsung
Chemistry	NCA	NMC	LCO, NMC
V_{nom} (V)	3.6	3.6	3.7
C_{nom} (Ah)	2.5	3	2.6
Standard charge CC-CV	1.25A 4.2V 125mA	1.5A 4.2V 50mA	1.3A 4.2V 520mA

For a SNR of 10 dB. The method described in section 2.2 demonstrates superior robustness, achieving a 100% convergence rate, while the two-stage algorithm only reaches 81%. The algorithm fails to converge, when during the iterative optimisation process, two differentiation orders have exactly the same value. Then, a loss of observability occurs and the algorithm fails. When the algorithm of section 2.1 converges, it shows highly biased results on some parameters, whereas the algorithm of section 2.2 still exhibits unbiased results and low standard deviation.

4. Experimental results on real batteries

Both algorithms are applied in this section for estimating parameters of three commercial battery cells which characteristics are provided in Table 2.

4.1. Experimental setup

An electrochemical workstation constituted of a Biologic-BCS-815 galvanostat/potentiostat, is used to perform charge and discharge cycles. The input signal used for identification is the Pseudo-Random Binary Sequence (PRBS) of Fig.9 (b-c). Temperature variations are negligible for such short durations of experiment. These experiments are conducted twice on each battery cell (i) once with no relaxation time after the charging sequence of Fig.9 (a) and (ii) once with a relaxation time of 60 minutes. The latter experiment is considered to provide reference values for the estimated parameters, as the free response vanishes after the observed delay. The objectives of the former experiment are to apply:

- the output error system identification method that assume the presence of only the forced response, to show how biased it is,

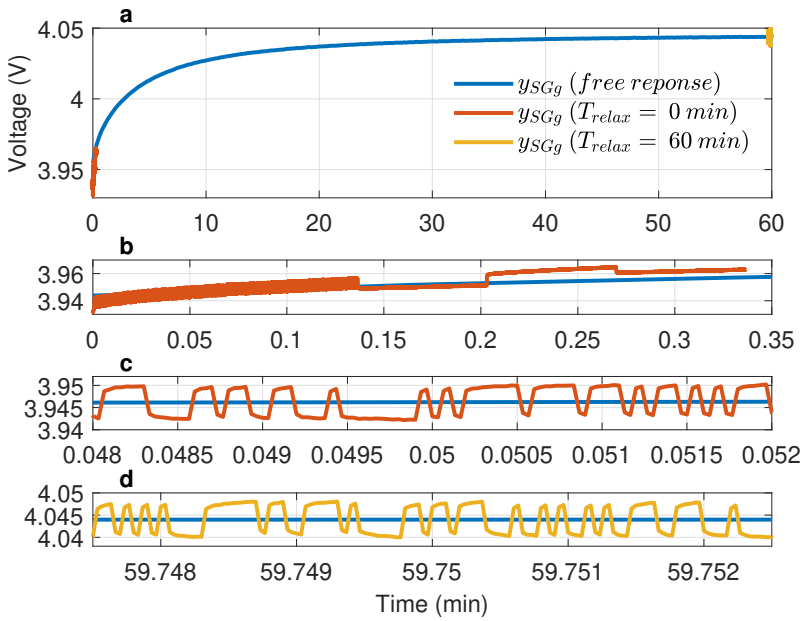

Figure 11: (a) Response of SGg cell to a PRBS input with no relaxation time (in red) and a PRBS with a relation time of 60 mn (in yellow). (b) Zoom of (a) in the indicated interval. (c) Zoom of (b) in the indicated interval. (d) Zoom of (a) in the indicated interval.

- the system identification algorithms with non-zero initial conditions developed in this paper to show that the bias is eliminated.

The input/output identification data obtained for one of the three cells are plotted in Fig.11 (data of other cells exhibit quite similar dynamics). This figure presents data from both experiments: without and with a 60-minute relaxation period. Validation input data are depicted in Fig.12(a).

4.2. Experimental results and discussion

The %fit is used as a metric. It is defined as

$$\%fit = \left(1 - \sqrt{\frac{E^T(\theta)E(\theta)}{y^T y}}\right) 100 \tag{33}$$

where the error vector $E(\theta) = [\epsilon(0,\theta), \ldots, \epsilon(K-1,\theta)]^T$ and ϵ is the output error from (20).

Fig. 12(b,c and d) and table 3 present the validation results on parameter estimation with both algorithms applied on the three battery cells. The obtained results using a relaxation period of 60 minutes ($\hat{\theta}_{60}$ in Table 12) have a $\%fit$ between 98.4 and 99.9%. Additionally, the results obtained using the two methods presented in this paper are compared to the one that uses the output error method by considering that the whole output is due only to the forced response as in [36]. In the latter case, the parameter estimation is very biased (see $\hat{\theta}_0^0$ in Table 12) and its corresponding %fit is the worse which explains why a quite long relaxation period is usually observed in the literature prior to data acquisition. Both algorithms developed in this paper perform quite well with a higher %fit rate for the second algorithm, also confirmed on Fig. 12. Additionally, the second algorithm has closer parameters to the ones computed by observing 60mn relaxation period, which provides another way for validating the performance of the proposed algorithms.

It is evident that taking the free response (algorithm of section 2.2) into account significantly improves the identification results. Hence, the proposed algorithms eliminate the need to wait for the system free response to decay, which is even more important in the case of fractional systems which decay polynomially, as compared to the exponential decal of rational systems. Hence, the relaxation period traditionally observed in battery systems prior to collecting identification/validation data can now be squeezed. Both algorithms have successfully been applied to all three commercial battery cells and the identified parameters were quite close to the ones estimated after a relaxation time of 60mn, which allows asserting that the algorithms are performant.

5. Conclusions

This paper introduces two novel algorithms for system identification using fractional models with non-zero initial conditions. To the best of authors' knowledge, no such algorithm has ever been proposed in the literature. It has been shown using Monte Carlo simulation and on real data that both algorithms perform well, with a slight superiority of the one-stage algorithm, described in section 2.2, as compared to the the two-stage algorithm, of section 2.1. The main reason is that the former algorithm uses both the free and the forced responses for parameter estimation, whereas the latter isolates the forced response which is then used for parameter estimation.

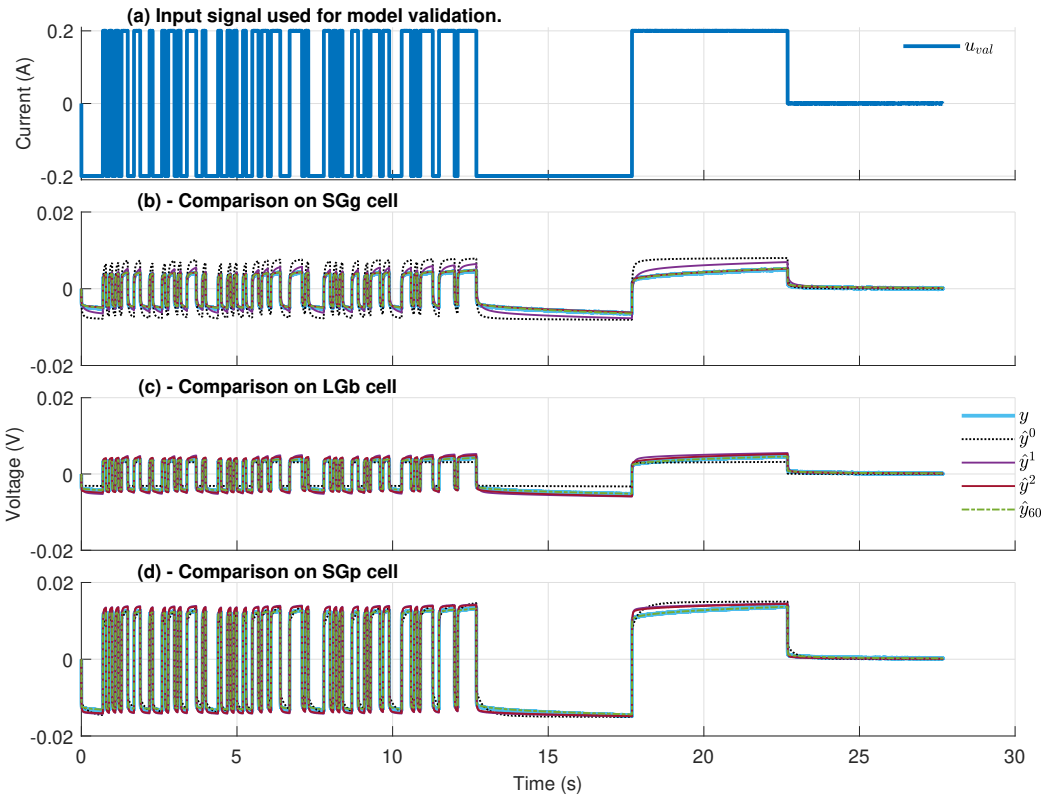

Figure 12: Comparison on validation data between system output y, model output considering that the whole output is due only to the forced response, ($\hat{y}^0$), model output obtained by the algorithm of section 2.1 ($\hat{y}^1$), model output obtained by the algorithm of section 2.2($\hat{y}^2$), and model output obtained using a relaxation period of 60min ($\hat{y}$).

Table 3: Comparison of parameter estimation accuracy with and without a relaxation period of 60 min for various battery cells using different methods. $\hat{\theta}_{60}$ refers to the results obtained with a 60-minute relaxation period, $\hat{\theta}_0^0$ refers to results obtained without relaxation model output considering that the whole output is due only to the forced response, $\hat{\theta}_0^1$ refers to results obtained using the method described in section 2.1, and $\hat{\theta}_0^2$ refers to results obtained using the method described in section 2.2.

Cell ref	SGg				LGb				SGp			
Parameters	$\hat{\theta}_{60}$	$\hat{\theta}_0^0$	$\hat{\theta}_0^1$	$\hat{\theta}_0^2$	$\hat{\theta}_{60}$	$\hat{\theta}_0^0$	$\hat{\theta}_0^1$	$\hat{\theta}_0^2$	$\hat{\theta}_{60}$	$\hat{\theta}_0^0$	$\hat{\theta}_0^1$	$\hat{\theta}_0^2$
R_0 (mΩ)	14.2	14.25	14.2	14.2	15.1	15.3	15.1	15.1	49.5	50	49.5	49.5
R_{ct} (mΩ)	7.9	25.8	18	7.8	3.5	0.36	3.2	6.5	12.2	18.4	19.8	18.6
Q_{dl} (F.s$^{1-\alpha}$)	6.81	3.1	10.75	5.98	1.42	3.37	4.8	1.4	0.45	16.33	1.13	0.83
α	0.67	0.66	0.67	0.66	0.88	0.73	0.88	0.88	0.86	0.89	0.86	0.86
Q_d (F.s$^{1-\beta}$)	301	4000	437	340	348	3998	518	348	230	148	478	391
β	0.65	0.61	0.65	0.65	0.53	0.72	0.53	0.53	0.48	0.008	0.48	0.48
$\%fit_{identif}$	98.4	37.3	92.5	94.7	99.57	60.89	96.1	98.2	98.5	17.40	94.9	96.3
$\%fit_{val}$	99.7	63.9	94.6	99.7	99.9	80.94	96.7	98.7	99.9	89.9	99.3	99.5

It has been shown that the algorithms are particularly useful in Li-ion battery cells identification, as they allow to completely eliminate the relaxation time, usually observed when a battery is driven to a given SOC-level.

References

[1] L. Lai, Y.-D. Ji, S.-C. Zhong, L. Zhang, Sequential parameter identification of fractional-order duffing system based on differential evolution algorithm, Mathematical Problems in Engineering 2017 (1) (2017) 3572365. doi:10.1155/2017/3572365.

[2] B. Wang, S. E. Li, H. Peng, Z. Liu, Fractional-order modeling and parameter identification for lithium-ion batteries, Journal of Power Sources 293 (2015) 151–161. doi:10.1016/j.jpowsour.2015.05.059.

[3] J.-D. Gabano, T. Poinot, H. Kanoun, Lpv continuous fractional modeling applied to ultracapacitor impedance identification, Control Engineering Practice 45 (2015) 86–97. doi:10.1016/j.conengprac.2015.09.001.

[4] S. Victor, R. Malti, H. Garnier, A. Oustaloup, Parameter and differentiation order estimation in fractional models, Automatica 49 (4) (2013) 926–935. doi:10.1016/j.automatica.2013.01.026.

[5] C. Lorenzo, T. Hartley, Initialization of fractional-order operators and fractional differential equations, Journal of computational and nonlinear dynamics. Special issue on discontinuous and fractional dynamical systems 3 (2008) 021101–1, 021101–9. doi:10.1115/1.2833585.

[6] J.-C. Trigeassou, N. Maamri, Initial conditions and initialization of linear fractional differential equations, Signal Processing 91 (3) (2011) 427–436. doi:10.1016/j.sigpro.2010.03.010.

[7] B. Du, Y. Wei, S. Liang, Y. Wang, Estimation of exact initial states of fractional order systems, Nonlinear Dynamics 86 (2016) 2061–2070. doi:10.1007/s11071-016-3015-7.

[8] J.-C. Trigeassou, N. Maamri, Analysis, modeling and stability of fractional order differential systems 1, ISTE Ltd, Wiley, London, 2019.

[9] Z. Wang, G. Feng, X. Liu, F. Gu, A. Ball, A novel method of parameter identification and state of charge estimation for lithium-ion battery energy storage system, Journal of Energy Storage 49 (February) (2022) 104124. doi:10.1016/j.est.2022.104124.

[10] A. Adel, R. Malti, O. Briat, Hybrid state of charge estimator for a lithium-ion battery based on a fractional model and fuzzy logic, IFAC-PapersOnLine 58 (12) (2024) 454–459, 12th IFAC Conference on Fractional Differentiation and its Applications ICFDA 2024. doi:10.1016/j.ifacol.2024.08.233.

[11] H. Wang, M. Tahan, T. Hu, Effects of rest time on equivalent circuit model for a li-ion battery, Proceedings of the American Control Conference 2016-July (2016) 3101–3106. doi:10.1109/ACC.2016.7525394.

[12] A. Barai, G. H. Chouchelamane, Y. Guo, A. McGordon, P. Jennings, A study on the impact of lithium-ion cell relaxation on electrochemical impedance spectroscopy, Journal of Power Sources 280 (2015) 74–80. doi:10.1016/j.jpowsour.2015.01.097.

[13] M. Messing, T. Shoa, S. Habibi, Lithium-ion battery relaxation effects, 2019 IEEE Transportation Electrification Conference and Expo (ITEC) 1 (2019) 1–6. doi:10.1109/ITEC.2019.8790449.

[14] T. Poinot, J.-C. Trigeassou, A method for modelling and simulation of fractional systems, Signal processing 83 (2003) 2319–2333. doi:10.1016/S0165-1684(03)00185-3.

[15] V. Martynyuk, M. Ortigueira, Fractional model of an electrochemical capacitor, Signal Processing 107 (2015) 355–360. doi:10.1016/j.sigpro.2014.02.021.

[16] C. F. Lorenzo, Initialized Fractional Calculus, NASA Glenn Research Center, 2000.

[17] T. T. Hartley, C. F. Lorenzo, J.-C. Trigeassou, N. Maamri, Equivalence of history-function based and infinite-dimensional-state initializations for fractional-order operators, Journal of Computational and Nonlinear Dynamics 8 (4) (jun 2013). doi:10.1115/1.4023865.

[18] S. Cruz-Manzo, P. Greenwood, An impedance model based on a transmission line circuit and a frequency dispersion warburg component for the study of eis in li-ion batteries, Journal of Electroanalytical Chemistry 871 (2020) 114305. doi:10.1016/j.jelechem.2020.114305.

[19] P. L. dos Santos, T.-P. A. Perdicoúlis, P. A. Salgado, Identification of optimal prediction error thévenin models of li-ion cells using the moli approach, arXiv e-prints 1 (2022) 1–25. arXiv:2212.09452, doi:10.48550/arXiv.2212.09452.

[20] R. Malti, X. Moreau, F. Khemane, A. Oustaloup, Stability and resonance conditions of elementary fractional transfer functions, Automatica 47 (11) (2011) 2462–2467. doi:10.1016/j.automatica.2011.08.029.

[21] T. S. Aghdam, S. M. M. Alavi, M. Saif, Structural identifiability of impedance spectroscopy fractional-order equivalent circuit models with two constant phase elements, Automatica 144 (2022) 110463. doi:10.1016/j.automatica.2022.110463.

[22] O. Arahbi, B. Huard, J. D. Gabano, T. Poinot, Automatic initialization of a complex nonlinear least squares algorithm for impedance battery frequential identification, Journal of Energy Storage 73 (PD) (2023) 109149. doi:10.1016/j.est.2023.109149.

[23] A. Nasser-Eddine, B. Huard, J.-D. Gabano, T. Poinot, A two steps method for electrochemical impedance modeling using fractional order system in time and frequency domains, Control Engineering Practice 86 (2019) 96–104. doi:10.1016/j.conengprac.2019.03.001.

[24] A. Nasser-Eddine, B. Huard, J. D. Gabano, T. Poinot, S. Martemianov, A. Thomas, Fast time domain identification of electrochemical systems at low frequencies using fractional modeling, Journal of Electroanalytical Chemistry 862 (2020) 113957. doi:10.1016/j.jelechem.2020.113957.

[25] S. M. Alavi, C. R. Birkl, D. A. Howey, Time-domain fitting of battery electrochemical impedance models, Journal of Power Sources 288 (2015) 345–352. doi:10.1016/j.jpowsour.2015.04.099.

[26] A. Adel, R. Malti, O. Briat, Time-domain system identification of li-ion batteries from non-zero initial conditions, IFAC-PapersOnLine 56 (2) (2023) 6111–6116, 22nd IFAC World Congress. doi:10.1016/j.ifacol.2023.10.707.

[27] A. Oustaloup, La dérivation non-entière: théorie, synthèse et applications, Hermès - Paris, 1995.

[28] R. Malti, S. Victor, Crone toolbox for system identification using fractional differentiation models, IFAC-PapersOnLine 48 (28) (2015) 769–774. doi:10.1016/j.ifacol.2015.12.223.

[29] D. Theuerkauf, L. Swan, Characteristics of open circuit voltage relaxation in lithium-ion batteries for the purpose of state of charge and state of health analysis, Batteries 8 (8) (2022). doi:10.3390/batteries8080077.

[30] T. Poinot, J.-C. Trigeassou, Identification of fractional systems using an output-error technique, Nonlinear Dynamics 38 (1-4) (2004) 133–154. doi:10.1007/s11071-004-3751-y.

[31] R. Malti, S. Victor, A. Oustaloup, Advances in system identification using fractional models, Journal of Computational and Nonlinear Dynamics 3 (2008) 021401–1. doi:10.1115/1.2833910.

[32] D. W. Marquardt, An algorithm for least-squares estimation of nonlinear parameters, J. Soc. Indust. Appl. Math. Vol. 11. No. 2, June, 1963 11 (51) (1963) 431–441. doi:10.1137/0111030.

[33] W. Spinelli, L. Piroddi, M. Lovera, A two-stage algorithm for structure identification of polynomial narx models, 2006 American Control Conference 1 (2006) 6–pp. doi:10.1109/ACC.2006.1656577.

[34] Z. Jiao, Z. Gao, H. Chai, S. Xiao, K. Jia, An adaptive unscented particle filter for a nonlinear fractional-order system with unknown fractional-order and unknown parameters, Signal Processing 220 (January 2024) (2024) 109443. doi:10.1016/j.sigpro.2024.109443.

[35] F. Bianchi, M. Prandini, L. Piroddi, A randomized two-stage iterative method for switched nonlinear systems identification, Nonlinear Analysis: Hybrid Systems 35 (2020) 100818. doi:10.1016/j.nahs.2019.100818.

[36] A. Adel, R. Malti, J.-M. Vinassa, O. Briat, Time-domain versus frequency-domain system identification of lithium-ion batteries using fractional models, IFAC-PapersOnLine 58 (15) (2024) 109–114, 20th IFAC Symposium on System Identification SYSID 2024. doi:10.1016/j.ifacol.2024.08.513.

Manuscript.tex

Figure_4

Click here to access/download;Figure;figure4_GEIS2.eps

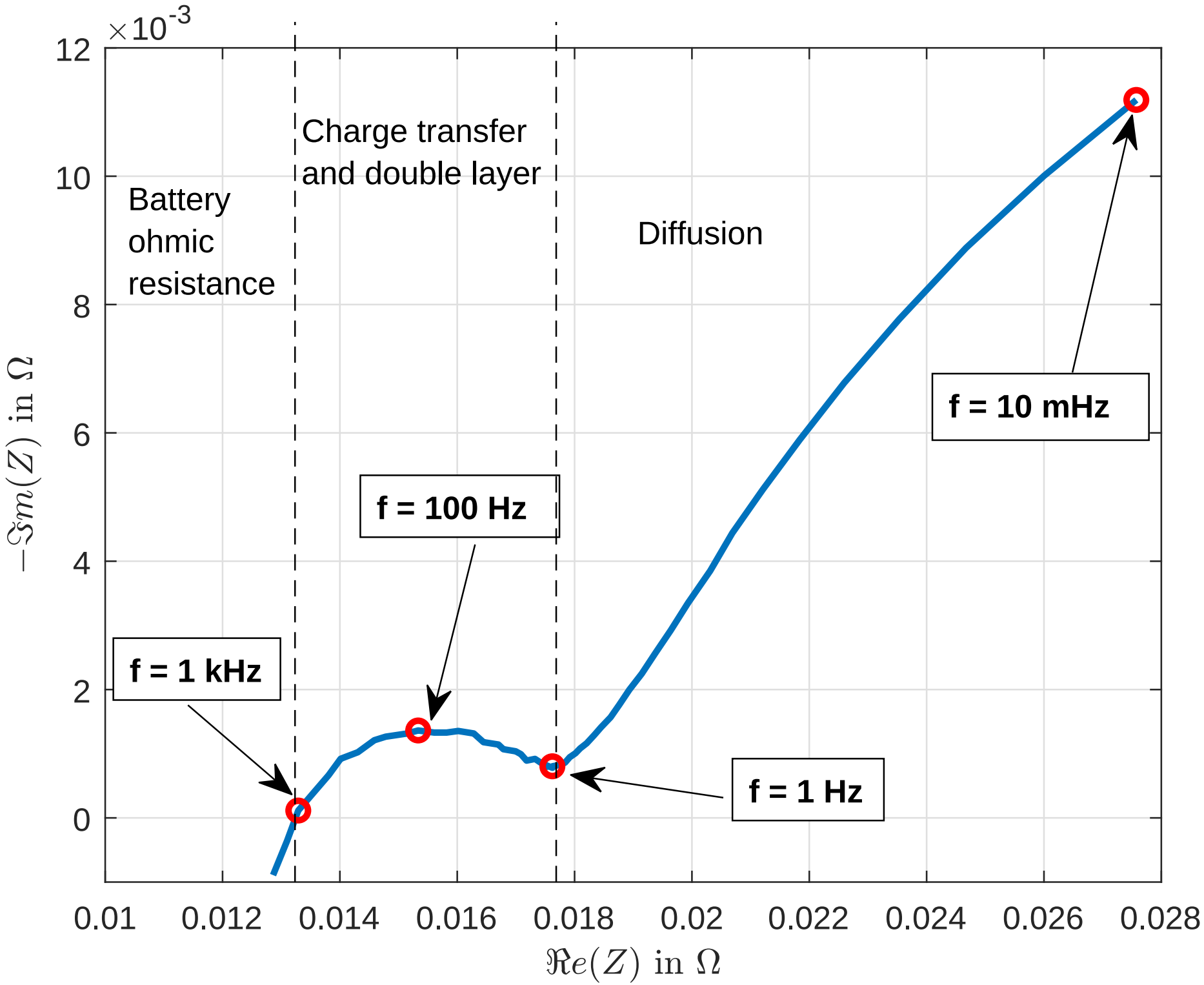

Figure_9

Click here to access/download;Figure;figure9_input.eps

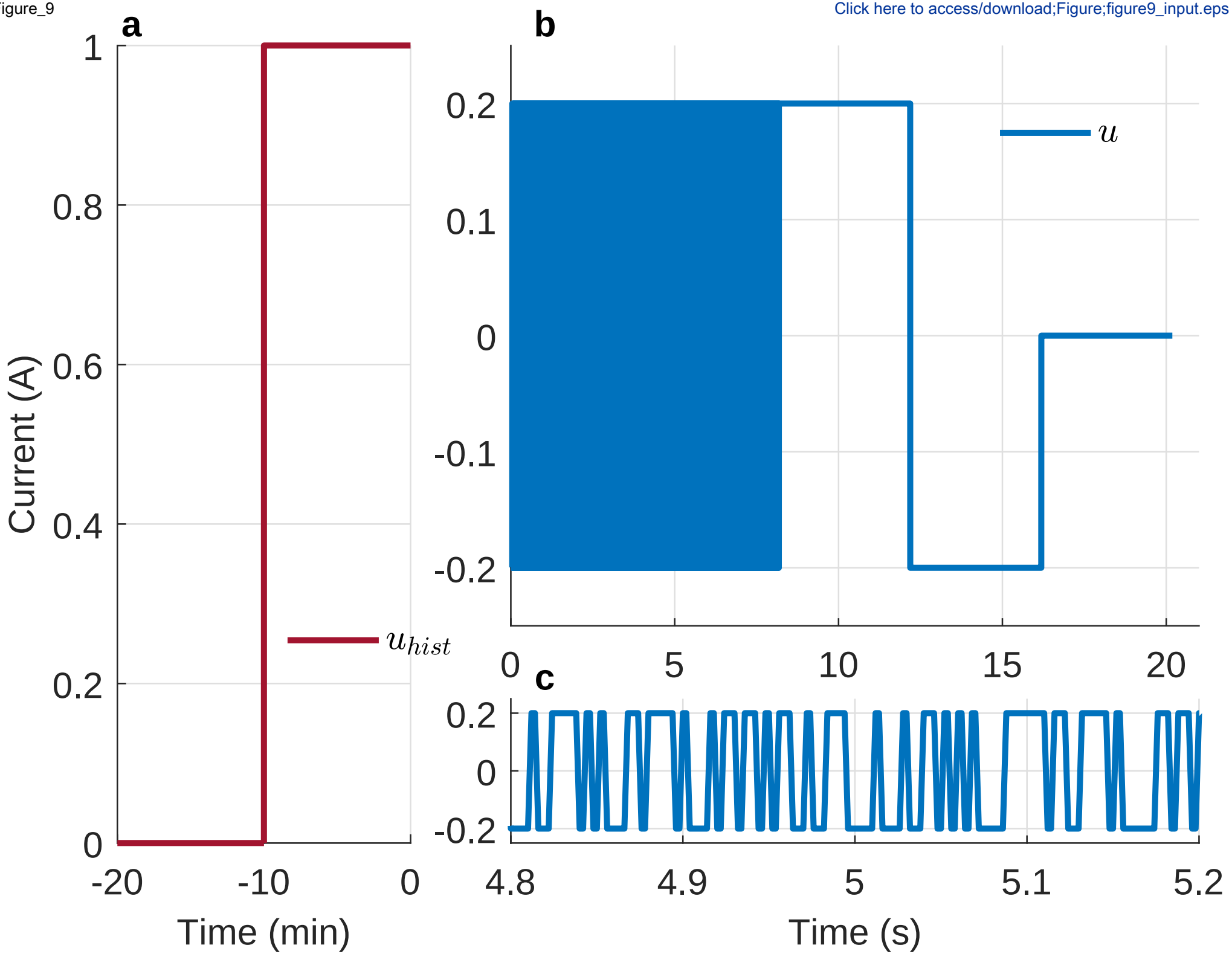

Figure_10

Click here to access/download;Figure;figure10_Simrelax0.eps

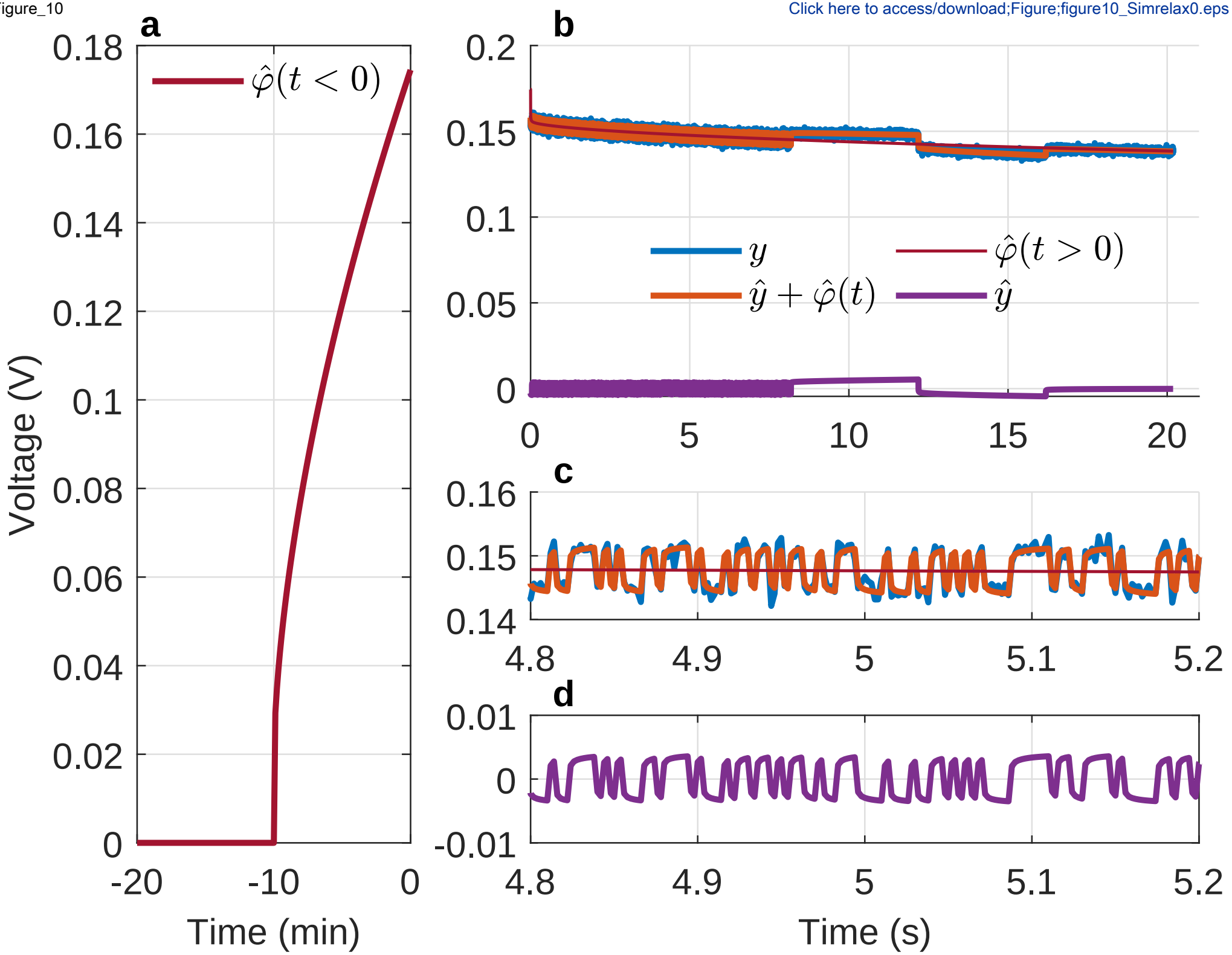

Figure_11

Click here to access/download;Figure;figure11_SGgdata1.eps

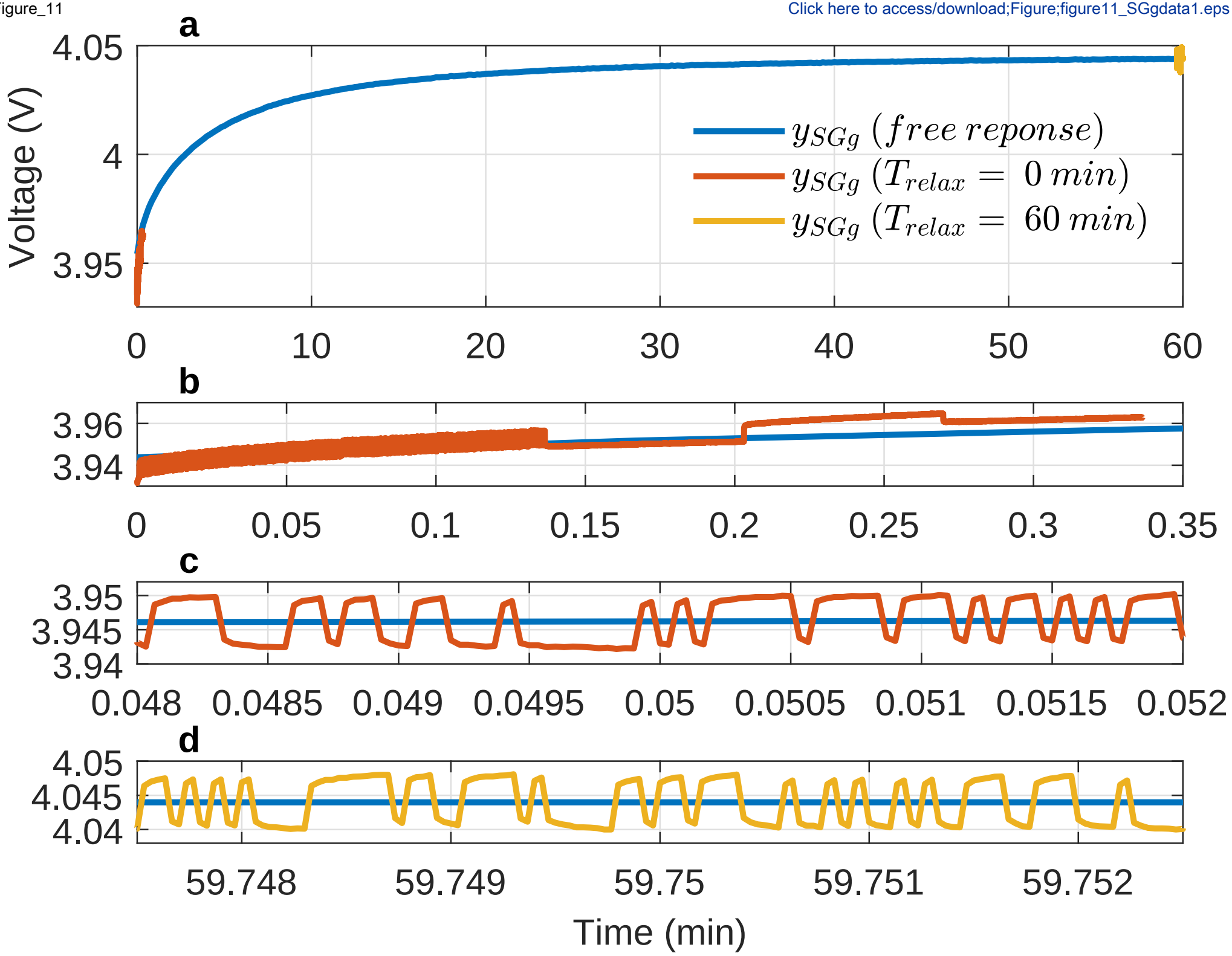

Figure_12

Click here to access/download;Figure;figure12_tech1and2timevalandinput.eps

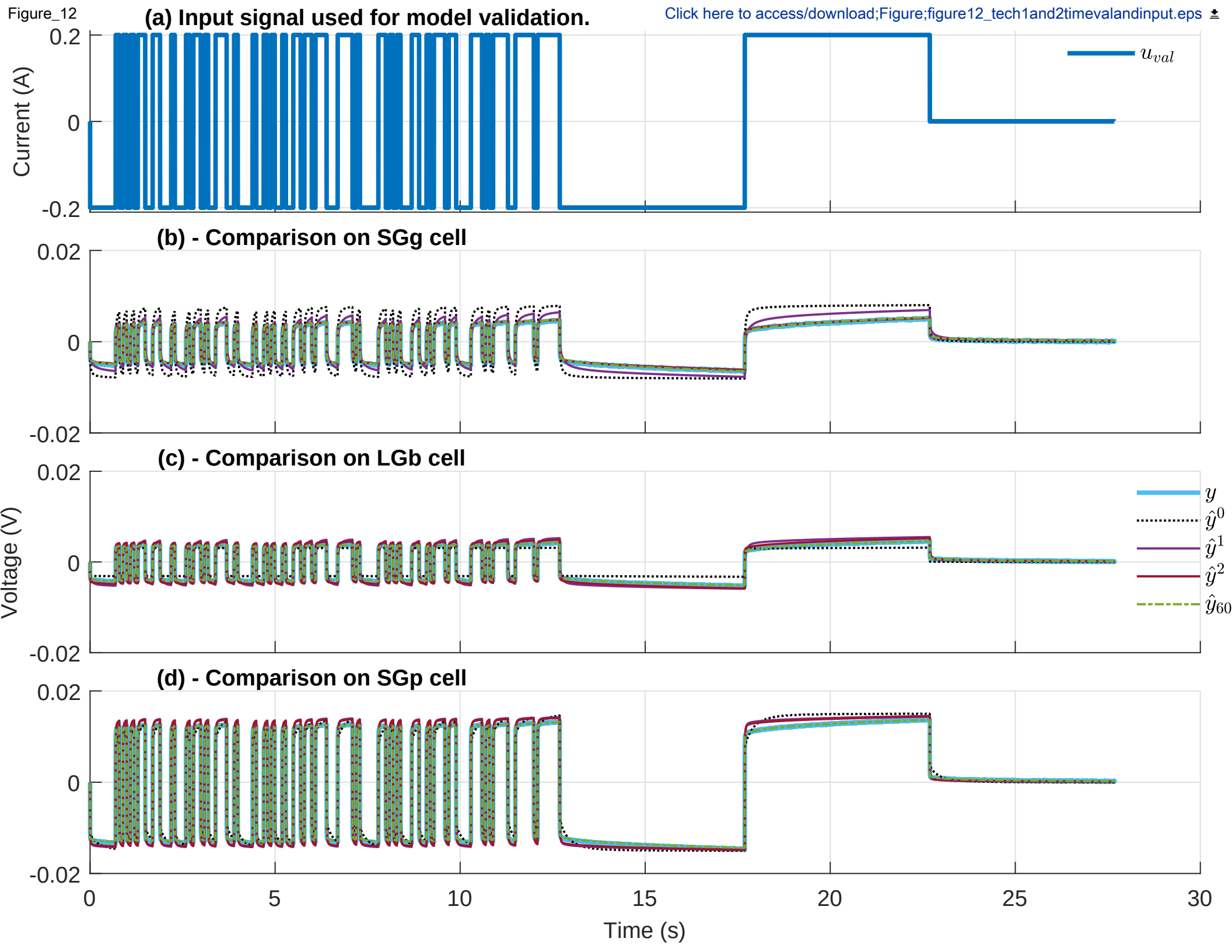

References List LaTeX Source Files

Click here to access/download

LaTeX Source Files

References.bib

Declaration of interests

☒The authors declare that they have no known competing financial interests or personal relationships that could have appeared to influence the work reported in this paper.

☐The authors declare the following financial interests/personal relationships which may be considered as potential competing interests: